A short overview on the use of optical satellite data in atmospheric corrections for satellite InSAR applications

Rosa Lasaponara, Antonio Lanorte

IMAA-CNR, EARSeL General Secretary, , C/da S. Loya Tito Scalo 85050 (PZ) İtaly
rosa.lasaponara@imaa.cnr.it

Abstract. SAR interferometric (InSAR) techniques allow us to estimate displacements of the earth's surface with a centimeter to millimetric precision InSAR techniques date back to 1989 when L-band SEASAT SAR data was first exploited to this aim and in the last few years the capability of different interferometric techniques has been considerably improved . Moreover, the finer spatial resolution and the short revisit time of the most recent satellite SAR, such as TERRA and COSMO-SkyMed constellations appear very promising for further significant improvements. Nevertheless, even if radar are all weather sensors it is also important to improve the estimation and minimization of effects of atmospheric delays. This paper provide a short overview on the use of optical satellite data in atmospheric corrections for satellite InSAR applications.

Keywords. INSAR, atmospheric phase delay, PWV, MODIS, MERIS, GPS

1. Introduction

SAR interferometric techniques allow us to estimate displacements of the earth's surface with a centimeter to millimetric precision by exploiting the difference in the phase values computed for two or more SAR images acquired for the study area at different times. As known, the difference in the interferometric phase (i.e difference in the signal path between two or more acquisitions) depends not only on the differences in elevation between the two or more images, but also by a number of additional contributions, described in equation 1, including orbital parameters, weather conditions and a noise component.

$$\Delta\phi = \Delta\phi_{topo} + \Delta\phi_{mov} + \Delta\phi_{orb} + \Delta\phi_{atm} + \Delta\phi_{noise} \quad \text{eq. 1}$$

For most applications, with particular reference to the estimation and monitoring of soil slow movements, it is necessary to estimate and remove (or at least minimize) the impact of “additional” contributions. In particular, the discrimination in a differential interferogram of the atmospheric signal from that of deformation can be very complex since the signals of phase delay (caused by atmospheric water vapour) and those caused by deformations can be very similar in both amplitudes and spatial extensions.

Several authors (eg , Goldstein, 1995; Zebker et al., 1997; Hanssen, 1998, Li et al. 2006a, 2009; Ding et al., 2008) have studied in detail the atmospheric effects on InSAR. Results from these studies, pointed out that changes in atmospheric relative humidity at around 20% may introduce errors up to 10-14 cm in the estimation of ground deformations and also significant errors (around 80-290 m) in topographical maps. Therefore, when the focus of the analysis is the estimation and monitoring of slow movements of the soil using a time series of images (usually taken in conditions very different from each other), it is necessary to mitigate the effects of phase delay.

2. Atmospheric delay

Atmospheric delay which may affects radar signal is mainly due to the spatial heterogeneity of tropospheric water vapor. Currently there are different methods to estimate and reduce the atmospheric effects in the InSAR applications. These approaches can be divided into four main types methods based on:

1 . Stacking SAR interferograms (see, for example, Zebker et al., 1997, Williams et al. 1998) which degrade the temporal resolution of the DInSAR measures and tend to mix useful geophysical signals, in particular transient signals, making them undetectable.

2 . Analysis of correlation between interferograms or between the interferometric phases and elevations (for example, adopted Beauducel et al., 2000; Fruneau and Sarti, 2000, Remy et al. 2003; Chaabane et al., 2007). These thecniques allow us to only model and reduce lower tropospheric noise which correlates different interferograms or with significant values in elevation

3 . Techniques based on permanent scatterer (PS) (see for example, Ferretti et al., 2000; Hoo -per et al. 2004). PS techniques require a large number of images, and do not provide satisfactory results when atmospheric effects are similar (in the spatial or temporal domain) to geophysical signals.

4 . Techniques based on the use of external data, such as (i) meteorological data (Delacourt et al. , 1998), (ii) GPS (Li et al 2006a,b,c; Li et al 2006d), (iii) high resolution meteorological models (Webley et. al 2004, Foster et al., 2006) and (iv) satellite data, such as MODIS (Moderate Resolution Imaging Spectroradiometer) (Li, 2005, Li et al. 2005) and/or MERIS (Medium Resolution Imaging Spectrometer) (Li et al., 2006c ; Li et al., 2009).

Among the above quoted approaches, great attention has been devoted to the use of satellite-based Precipitable Water Vapour (PWV) products due to the technical improvements achieved in the last years in terms of resolution and accuracy. Both MODIS and MERIS PWV products have been (eg. Li, 2005; Li et al., 2005; Li et al., 2006c ; Puysségur et al., 2007; Ding et al. , 2008; Li et al., 2009) adopted for atmospheric correction in InSAR techniques. In particular, PWV MERIS products have been most investigated mainly because MERIS data: (i) were available simultaneously with ASAR (being both sensors aboard ENVISAT), (ii) provide PWV estimation in spatial resolution up to 0.3 km (much higher than other data sources) and with an accuracy close to that of GPS (with a difference of about 1.1 mm rms). For these reasons, MERIS PWV products are considered to be very promising to correct atmospheric effects in the ASAR interferograms.

Li et al (2006b) quantitatively evaluated the impact of PWV MERIS in atmospheric corrections applied for ASAR interferometric chain for Los Angeles (Li et al., 2006c) and Hong Kong (Ding et al. 2008).

Puysségur et al (2007) proposed an atmospheric corrections techniques based on the integration of MERIS products with MM5 model (mesoscale meteorological model of the fifth generation developed by the National Center for Atmospheric Research/Pennsylvania State University). Quantitative evaluations carried out by Puysségur et al (2007) confirmed that the use of MERIS was highly satisfactory but no significant improvements were achieved using MERIS products jointly with MM5 model.

Li et al. (2009) proposed the combined use of MODIS and MERIS but, also in this case, the quantitative evaluation showed not significant improvement compared with the use of the sole MERIS.

Williams et al. (1998) have shown that in addition to the accuracy and the density of the data also the adopted interpolation model is critical.

3. Methods to compute atmospheric delay from PWV from MERIS/MODIS products

3.1. MERIS and MODIS water vapor data

MERIS, mounted with the ASAR on the space platform ENVI -SAT European Space Agency, is an optical sensor that measures the solar radiation reflected by the Earth's surface and clouds. However, on April 8, 2012, after 10 years in orbit, communication with the Envisat satellite was suddenly lost, and was later declared the end of the mission.

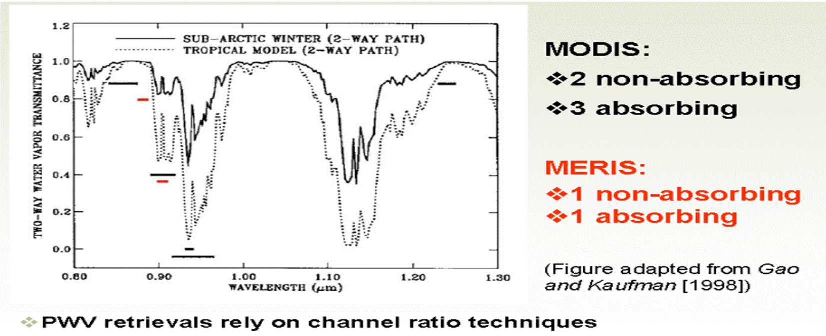

Figure 1. MODIS/MERIS Channel Positions Related to PWV (from Gao and Kaufman, 1998)

Products	GPS PWV	MODIS near IR PWV	MERIS near IR PWV
Number of Satellites	≥24	2	1
Coverage*	Regional	Global	Global
Observation Period	Day and night	Day	Day
Spatial Resolution*	A few km to a few hundred km (e.g. 10 km to 25 km over SCIGN)	1 km × 1 km	RR: 1.2km × 1.2km FR: 300m × 300m
Temporal Resolution	Almost continuous (e.g. 5 minutes)	Up to 4 times at some latitudes during daytime	3 days
Sensitivity to Clouds	No	Yes	Yes
PWV Accuracy	~1 mm	5-10% (or 1.6~2.0 mm)	1.6~2.0 mm

*: Both coverage and spatial resolution are relative to current CGPS networks in the world.

GPS, MODIS and MERIS PWV products are complementary!

Figure 2. Comparison of PWV products from satellite and GPS (UCL courtesy)

The images cover a range of 1150 km (nominal altitude of 800 km) and allow seamless global coverage in two or three days. MERIS has 15 spectral bands from the visible to the near infrared (390-1040 nm). Two of the 15 spectral bands in the near infrared, in an absorption band (885 nm) and the other outside of the absorption band (900 nm), are used to calculate maps of PWV using the method of differential absorption .

MODIS (Moderate Resolution Imaging Spectroradiometer) is a spectroradiometer which provides data with high radiometric sensitivity (12 bit) in 36 spectral bands with wavelengths from visible to thermal infrared with a spatial resolution ranging from 250 m 1 km away. The near- IR water vapor products provided by MODIS have a spatial resolution of 1 km × 1 km (at nadir) and are widely used for almost a decade for the correction of the atmospheric effects on InSAR data. The algorithm used to calculate the amount of water vapor is based on observations of water vapor attenuation of solar radiation in the near-IR reflected from the earth's surface and by clouds. The measurements can be performed only on areas that have reflective surfaces in the near-IR. The techniques applied using the relationship between the absorption of water vapor channels centered at 905 , 936 and 940 nm with the channels corresponding to the spectral windows centered at 865 and 1240 nm.

Example of MODIS-PWV obtained for the Basilicata region (Figure 3) and MERIS-PWV (Figure 4), for the same study area as for the MODIS products, are in figures 3 and 4 respectively.

.

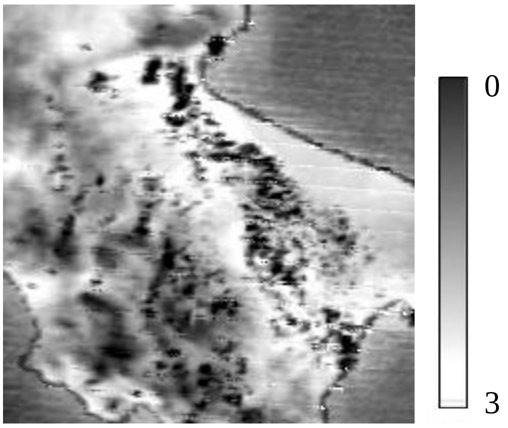

Figura 3. MODIS- PWV (cm)

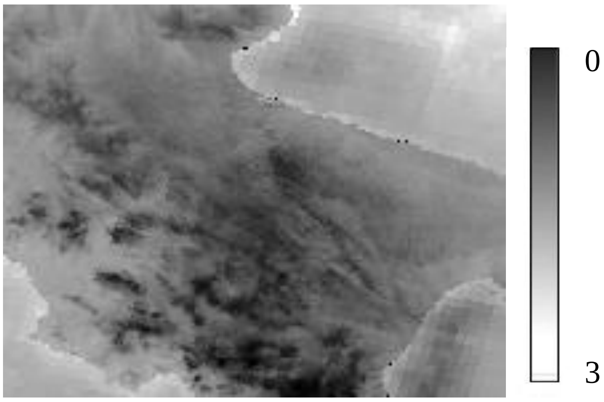

Figura 4. MERIS- PWV (cm)

3.2. Atmospheric phase delay correction

For the correction of the atmospheric delay, cloud-free (ie in the absence of cloud cover) PWV MODIS and MERIS products, must be converted into Zenith Wet Delay (ZWD) using equation 2

$$ZWD = \Pi \, PWV \qquad \text{eq. 2}$$

where Π denotes an adimensional parameter given by equation 3 (Bevis et al., 1994)

$$\pi = 10^{-6} \rho R_y \left[\frac{k_3}{T_m} + k_2 - wk1 \right] \qquad \text{eq. 3}$$

where ρ is the density of liquid water, Rv is the specific gas constant, K1, K2, K3 are constants of the atmospheric refractivity and w is the ratio of the mass of the molecules of water vapor and molecules of dry air; finally, T_m is the temperature-weighted average of the troposphere (eq. 4).

$$T_m = \frac{\int \left(e/T \right) dh}{\int \left(e/T^2 \right) dh} \qquad \text{eq. 4}$$

where *e* is the partial pressure of water vapor, T is the absolute temperature, and h is the height of the atmospheric profile.

The estimation of T_m from equation 4 is generally quite complex and difficult. Bevis et al. (1994) analyzed the relationship between the surface temperature T_o and T_m measured using a large number of radiosondes for North America. They found a high linear correlation between T_m and T_o with an RMS error at around 4.7 K.

$$T_m = 70.2 * 0.72\, T_o \qquad \text{eq. 5}$$

Assuming, T_o = 300k and a PWV= 2.0 cm, we have an error at around 4.7K on T_m due to an uncertainty of the order 0099 in the mapping of the scale factor Π. This introduces an error at around 1.98 mm in the estimation of ZWD. The impact of this error is absolutely negligible.

In its simplest form, the value of the Π conversion factor can be obtained by using equation 6 [Scheuler et al., 2001]

$$\Pi = 0.10200 + \frac{1708.08[K]}{T_M} \qquad \text{eq. 6}$$

T_m is generally obtained by using radiosonde profiles or using measurements of the superficial temperatures (from equation 5).

In the case of unavailability of radiosondes profiles or measurements of surface temperature the Π conversion factor can be, as suggested by Li et al. (2004), equal to 6.0 (for summer months), 6.2 (winter months), 6.1 (spring and autumn). Figures 5 and 6 show two examples of ZWD map from MODIS-PWV and MERIS-PWV.

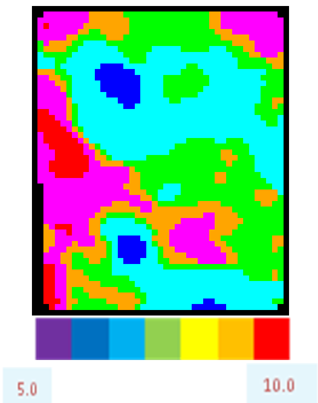

Figure 5.
MODIS- ZWD – April 10, 2011

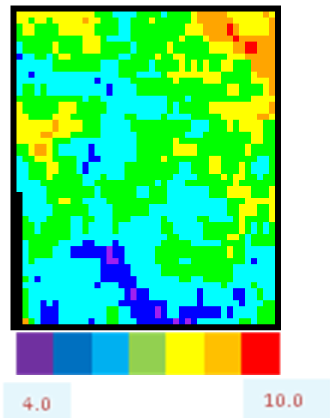

Figure 6.
MERIS-ZWD- April 3, 2011

Finally, ZPDDM is calculated as the difference between 2D ZWD fields. ZPDDM maps are further processed to “re-fill” cloudy pixels and eliminate calibration errors and/or noise using: (i) an interpolation method based on inverse distance weighing to fill the pixels covered by clouds and, therefore, excluded (ii) low-pass filters to remove residual noise.

All the computation steps of the model for the calculation of atmospheric phase delay are summarized in figure 7.

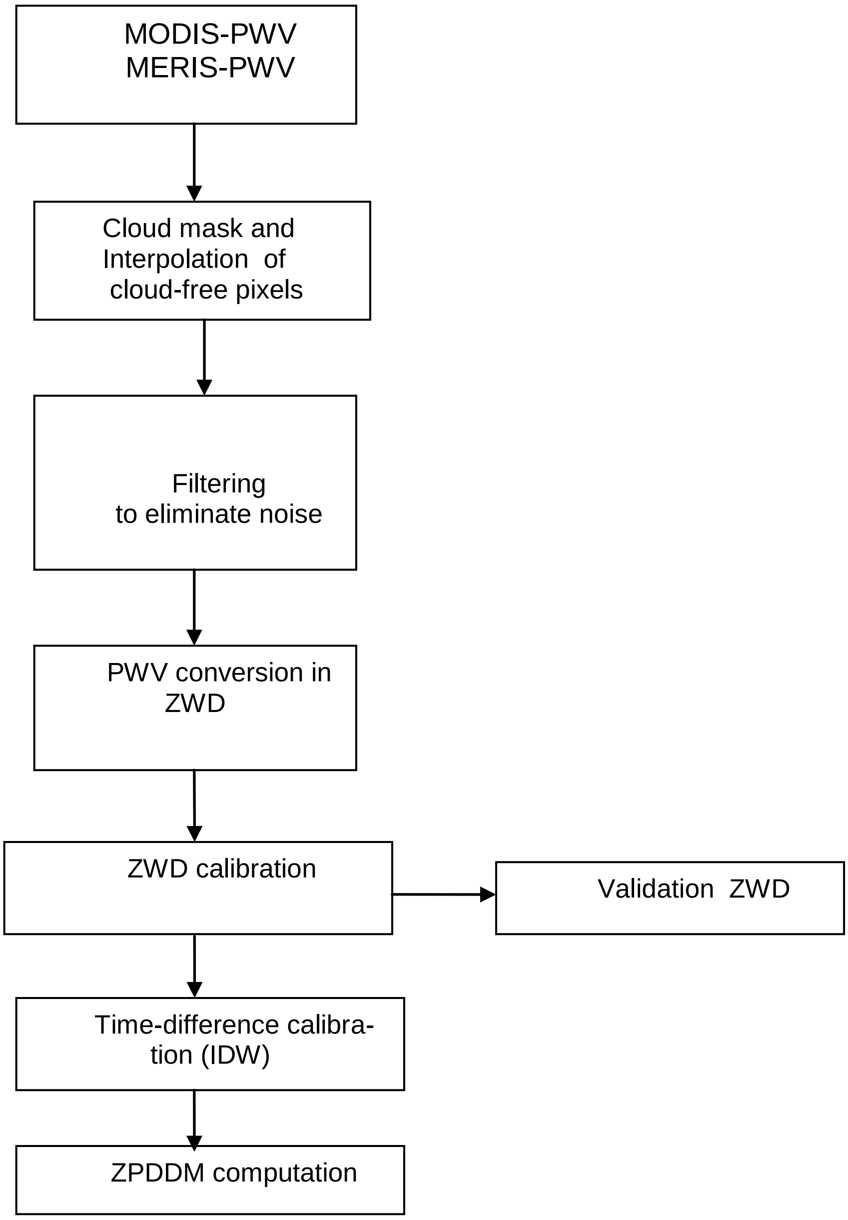

Figure 7. Flow chart adopted to obtain the wet delay from satellite data MODIS and MERIS

4. MODIS-ZWD e MERIS-ZWD calibration and validation

The calibration of the MODIS ZWD and MERIS ZWD is carried out using a procedure based on independent data source, mainly GPS or meteorological measurements (temperature and relative humidity). To this aim, the model developed by Saastamoinen (1972) based on temperature and relative humidity is generally considered reliable and accurate (Katsougiannopoulos et al., 2006) with an accuracy at around 3 cm at zenith (Mendes, 1999). The model, based on equation 7 assumes that the temperature decreases linearly with the height:

$$ZWD = 0.002277\left(\frac{1255}{T} + 0.05\right)e_0 \qquad \text{eq. 7}$$

where T is the atmospheric temperature in K (Kelvin)

e_0 is the unsatured vapour pressure in hPa obtained using the following equation:

$$e_o = 6.11(RH/100)10^{\frac{7,5 \cdot T}{237,7+T}} \qquad \text{eq. 8}$$

where RH is Relative Humidity.

For the investigated area located in the Basilicata region, we selected meterological measuremants, shown as yellow arrows in figure 8 and listed below, acquired at the same time as the MODIS e and MERIS imagery .

Potenza (40°37'35" - 15°47'49")

Oppido (40°45'49" - 15°59'08")

Marsico (40°25'35" - 15°43'46")

Albano (40°34'54" - 16°02'07")

The procedure compare the ZWD obtained from the Saastamoinen model with those obtained from satellite products (both MODIS-ZWD e MERIS-ZWD) which, according to Keeratikasikorn e Trisirisatayawong (2011) exhibit a linear relationship:

ZWDsaas_modis_time = a x ZWDmodis + b eq. 9

ZWDsaas_meris_time = a x ZWD meris + b eq. 10

Where $ZWD_{saas\_modis\_time}$ e $ZWD_{saas\_meris\_time}$ are ZWD obtained from the Saastamoinen model at the same time as the satelliet acqusition (for the study area MODIS at 10.00 UTC and MERIS at 9.00 UTC). ZWD_{modis} e ZWD_{meris} are ZWD obtained from MODIS-PWV and MERIS-PWV.

The scale facto a for both the equation 9 and 10 is obtained for the four stations and then spatially interpolated using Inverse Distance Weight (IDW) .

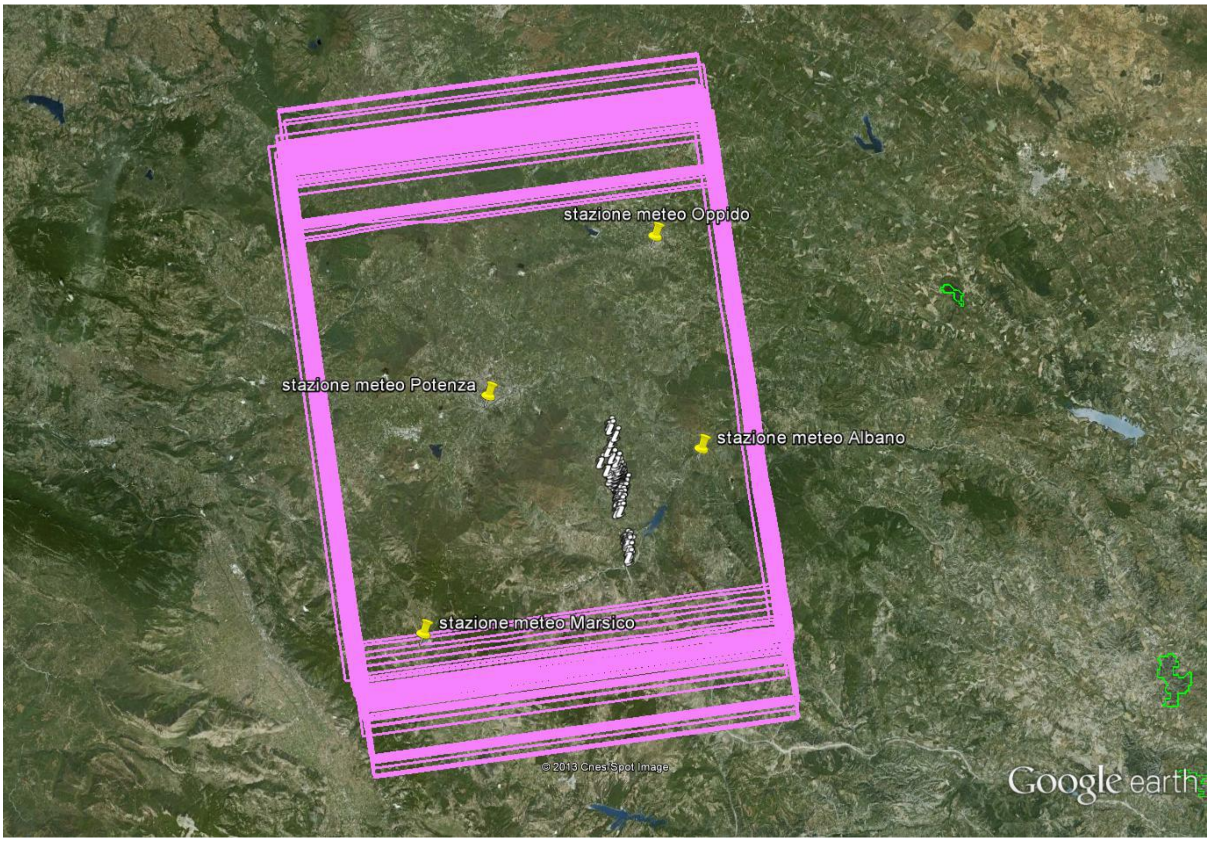

Figure 8. Yellow arrows indicate the positions of the meteorogical stations; pink boxes indicate the SAR frame

The validation procedure is performed by comparing the ZWD maps computed using the Saastamoinen (applied to a meteorological data sets different from those used for the calibration procedure) and the MODIS-ZWD e MERIS-ZWD maps calibrated as previously described.

Table 1 and 2 show the results of the comparison for MODIS and MERIS ZWD maps, respectively.

	Mod_ZWD pre-cal	Mod_ZWD post-cal
Correlation R^2	0.574	0.782
Error medium (cm)	2.42	2.05
Std. Dev. difference(cm)	1.97	1.56

Table 1. Validation of MODIS-ZWD before and after the calibration

	Mer_ZWD pre-cal	Mer_ZWD post-cal
Correlazione R^2	0.698	0.842
Errore medio (cm)	3.19	2.28
Std. Dev. differenze (cm)	2.32	1.79

Table 2. Validation of MERIS-ZWD before and after the calibration

Both table 1 and 2 clearly show that the correlation values are higher after the calibration phase R2 0.782 post-cal and 0.574 pre-cal for MODIS and R2 0.842 post-cal and 0.698 pre-cal for MERIS. The same behavior is observed for the errors 2.42 pre-cal cm to 2.05 cm post-cal and the standard deviation media from 1.97 cm pre-cal to1.56 cm post-cal. Similarly for the MERIS data set.

These results pointed out that the calibration procedure we adopted is suitable to correct the ZWD MODIS and MERIS products. The final point is to consider the difference in the time acquisition between SAR data and optical dataset (Figures 9 and 10). For the study area and the considered data sets, made up of COSMO SKYMED, MODIS and MERIS (2011) the difference in time acquisition is 5 hours for MODIS and 4 hours for MERIS, being that COSMO data acquired at around 5 pm. The estimation of the impact of non contemporaneity is performed considering the ZWD maps obtained from the Saastamoinen model applied to the meteorological data acquired at the same time as SAR data.

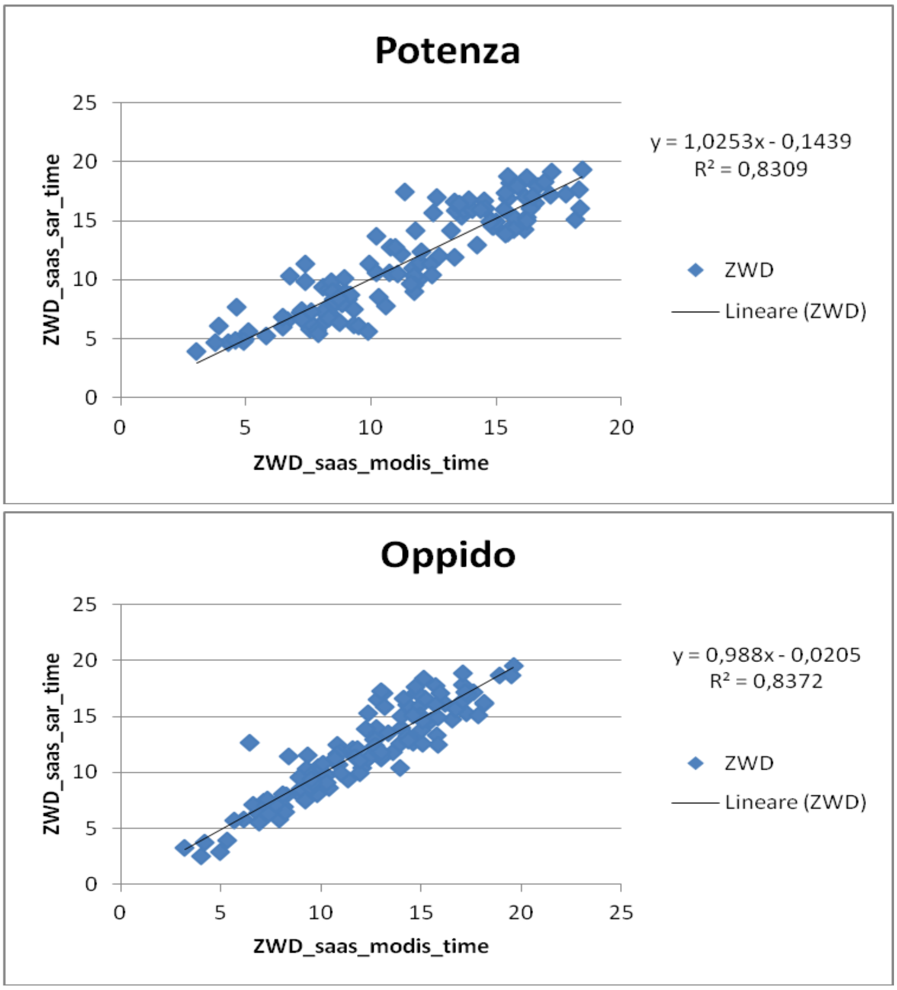

Figure 9. MODIS-ZWD time difference impact – Linear regression analysis (using two meteo stations)

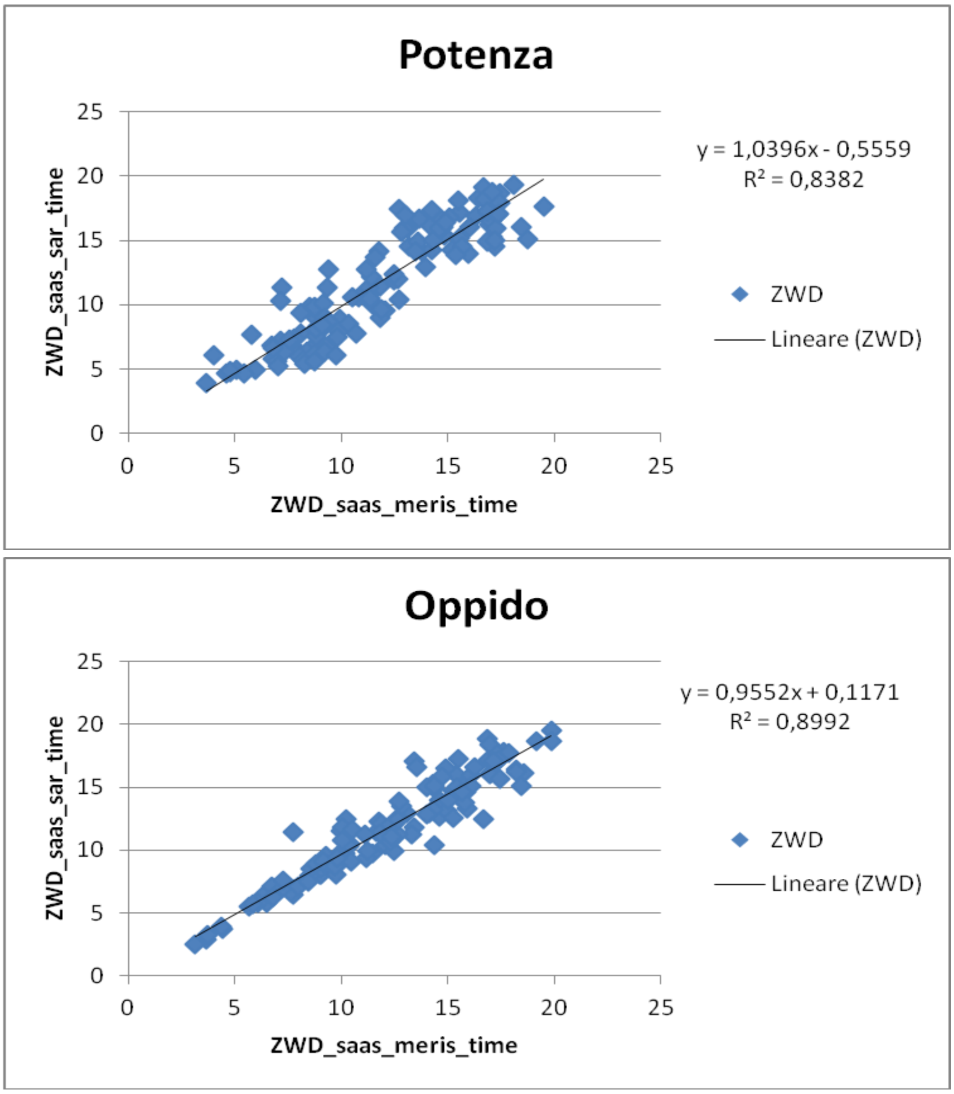

Figure 10. MERIS-ZWD time difference impact – Linear regression analysis (using two meteo stations)

5. Final Remarks

This paper provide a short overview on the use of optical satellite data in atmospheric corrections for satellite InSAR applications. Even if, being active sensors, satellite radars are all weather sensors for the acquisitin capability, it is important to remind that the effects of atmosphere tend to adversly impact the data introducing the socalled "atmospheric phase delay".

Over the years, several authors (eg , Goldstein 1995; Zebker et al 1997, Hanssen , 1998, Li et al. 2006b, 2007; Ding et al., 2008) have studied and quantified the atmospheric effects on InSAR. According to these studies, changes in atmospheric relative humidity at around 20% may introduce errors up to 10-14 cm in the estimation of ground deformations and also significant errors (around 80-290 m) in topographical maps. Therefore, when the focus of the analysis is the processing of a time series of images (usually taken in conditions very different from each other), it is necessary to mitigate the effects of phase delay.

In this paper we provide a short overview on the use of optical satellite data in atmospheric corrections for satellite InSAR applications. A procedure based on the use of satellite based PWV products is presented and discussed from the practical applications in the case study of a test sites in Basilicata region.

Acknowledgments

This work has been performed in the framework of the project " Analisi Critica Degli Algoritmi Allo Stato Dell'arte Per Correzioni Atmosferiche Da Dati Ottici Ed Indicazione Degli Algoritmi Selezionati" denoted as -SOS-MT-MONITORING-funded by the Italian Space Agency.

References

[1] Albert, P., R. Bennartz, and J. Fischer, Remote Sensing of Atmospheric Water Vapor from Backscattered Sunlight in Cloudy Atmospheres, Journal of Atmospheric and Oceanic Technology, 18 (6), 865-874, 2001.

[2] AMS, American Meteorological Society Glossary of Meteorology, Boston, Massachusetts, 2000.

[3] Askne, J., and H. Nordius, Estimation of tropospheric delay for microwaves from surface weather data, Radio Science, 22, 379-386, 1987.

[4] Beauducel, B., Briole, P. & Froger, J.L., 2000. Volcano-wide fringes in ERS synthetic aperture radar interferograms of Etna (1992–1998): deformation or tropospheric effect?, J. geophys. Res., 105, 16391–16402.

[5] Bennartz, R., and J. Fischer, Retrieval of columnar water vapour over land from back-scattered solar radiation using the Medium Resolution Imaging Spectrometer (MERIS), Remote Sensing of Environment, 78, 271-280, 2001.

[6] Bevis, M., S. Businger, T.A. Herring, C. Rocken, R.A. Anthes, and R. H. Ware, GPS meteorology: remote sensing of atmospheric water vapor using the Global Positioning System, Journal of Geophysical Research, 97 (D14), 15,787-15,801, 1992.

[7] Bevis, M., S. Businger, S. Chiswell, T. Herring, R. Anthes, C. Rocken, and R. Ware, GPS meteorology: mapping zenith wet delays onto precipitable water, Journal of Applied Meteorology, 33, 379-386, 1994

[8] Bézy, J.-L., S. Delwart, and M. Rast, MERIS - A new generation of ocean-colour sensor onboard Envisat, ESA Bulletin, 103, 48-56, 2000

[9] Chaabane, F., Avallone, A., Tupin, F., Briole, P. & Maıtre, H., 2007. A multitemporal method for correction of tropospheric effects in differential SAR Interferometry: application to the Gulf of Corinth Earthquake, IEEE Trans. Geosci. Remote Sens., 45, 1605–1615.

[10] Chaboureau, J.P., A. Chédin, and N. A. Scott, Remote sensing of the vertical distribution of the atmospheric water vapor from the TOVS observations: method and validation, Journal of Geophysical Research, 103 (D8), 8743-8752, 1998.

[11] Davis, J.L., T.A. Herring, I.I. Shapiro, A.E.E. Rogers, and G. Elgered, Geodesy by radio interferometry: Effects of atmospheric modeling errors on estimates of baseline length, Radio Science, 20, 1593-1607, 1985.

[12] Delacourt, C., Briole, P. & Achache, J., 1998. Tropospheric corrections of SAR interferograms with strong topography: application to Etna, Geophys. Res. Lett., 25(15), 2849–2852.

[13] Ding X-L, Li Z-W, Zhu J-J, Feng G-C, Long J-P. Atmospheric Effects on InSAR Measurements and Their Mitigation. *Sensors*. 2008; 8(9):5426-5448.

[14] Elgered, G., Tropospheric radio path delay from ground-based microwave radiometry, in Atmospheric Remote Sensing by Microwave Radiometry, edited by M. Janssen, pp. 215-258, John Wiley, New York, 1993

[15] Emardson, T.R., Studies of atmospheric water vapor using the Global Positioning System, Technical Report No. 339, Chalmers University of Technology, Goteborg, Sweden, 1998

[16] ESA-MERIS, MERIS Product Handbook, Issue 1.1 (available online at http://envisat.esa.int/dataproducts/meris/CNTR.htm), 2002

[17] Ferretti, A., Prati, C.&Rocca, F., 2000. Nonlinear subsidence rate estimation using permanent scatters in differential SAR interferometry, IEEE Trans.

[18] Fischer, J., and R. Bennartz, Retrieval of total water vapour content from MERIS measurements, ESA reference number PO-TN-MEL-GS-005, ESA-ESTEC, Noordwijk, Netherlands, 1997.

[19] Foster, J., Brooks, B., Cherubini, T., Shacat, C., Businger, S. & Werner, C., 2006. Mitigating atmospheric noise for InSAR using a high resolution weather model, Geophys. Res. Lett., 33, L16304, doi:10.1029/2006GL026781.

[20] Frouin, R., P.-Y. Deschamps, and P. Lecomte, Determination from space of atmospheric total water vapor amounts by differential absorption near 940 nm: Theory and airborne verification, Journal of Applied Meteorology, 29, 448-460, 1990

[21] Fruneau, B. and Sarti, F., 2000. Detection of ground subsidence in the city of Paris using radar interferometry: isolation of deformation from atmospheric artifact using correlation, Geophys. Res. Lett., 27, 3981–3984.
[22] Gao, B.C., and A.F.H. Goetz, Column atmospheric water vapor and vegetation liquid water retrievals from air-borne imaging spectrometer data, Journal of Geophysical Research, 95, 3549-3564, 1990
[23] Gao, B.C., and Y.J. Kaufman, ATBD-MOD-05: The MODIS near-IR water vapor algorithm (available online at: http://ltpwww.gsfc.nasa.gov/MODIS-Atmosphere/_docs/atbd_mod03.pdf), pp. 25, 1998
[24] Gao, B.C., and Y.J. Kaufman, Water vapor retrievals using Moderate Resolution Imaging Spectroradiometer (MODIS) near-infrared channels, Journal of Geophysical Research, 108 (D13), 4389, doi:10.1029/2002JD003023, 2003
[25] Goldstein, R. 1995. Atmospheric limitations to repeat-track radar interferometry. Geophys. Res. Lett.,22(18), 2517–2520.
[26] Hanssen, R. (1998). Atmospheric heterogeneities in ERS tandem SAR interferometry, chapter 2. Delft University Press, The Netherlands
[27] Hooper, A., Zebker, H., Segall, P., Kampes, B. (2004).A new method for measuring deformation on volcanoes and other natural terrains using InSAR persistent scatterers. Geophysical Research Letters, Vol. 31, L23611, doi:10.1029/2004GL021737, 2004
[28] Katsougiannopoulos, S., Pikridas, C., Rossikopoulos, D., Ifadis, I. M., & Fotiou, a. A. (2006). Tropospheric Refraction Estimation Using Various Models, Radiosonde Measurements and Permanent GPS data. XXIII FIG Congress. Munich, Germany
[29] Kaufman, Y.J., and B.C. Gao, Remote sensing of water vapor in the near IR from EOS/MODIS, IEEE Transactions on Geoscience and Remote Sensing, 30 (5), 871-884, 1992
[30] Keeratikasikorn C. and I. Trisirisatayawong, A Method to Use Modis Water Vapor Products For Correction of Atmospheric-Induced Phase in Interferogram. Artificial Satellites. Volume 46, Issue 2, Pages 47–62, 2011
[31] Li, Z.H., J.-P. Muller, and P. Cross,. Comparison of precipitable water vapor derived from radiosonde, GPS, and Moderate-Resolution Imaging Spectroradiometer measurements, Journal of Geophysical Research, 108 (D20), 4651, doi:10.1029/2003JD003372, 2003
[32] Li, Z., Correction of atmospheric water vapour effects on repeat-pass SAR interferometry using GPS, MODIS and MERIS data, PhD thesis, University College London,London, 2005
[33] Li, Z., J.-P. Muller, P. Cross, and E.J. Fielding, Interferometric synthetic apeture radar (InSAR) atmospheric correction: GPS, Moderate Resolution Imaging Spectroradiometer (MODIS), and InSAR integration, Journal of Geophysical Research, 110 (B3), B03410, doi:10.1029/2004JB003446, 2005
[34] Li, Z.H., Muller, J.P., Cross, P., Albert, P., Fischer, J. & Bennartz, R., 2006a. Assessment of the potential of MERIS near-infrared water vapour products to correct ASAR interferometric measurements, Int. J. Remote Sens., 27(2), 349–365.
[35] Li, Z.H., Fielding, E.J., Cross, P. & Preusker, R., 2009. Advanced InSAR atmospheric correction: MERIS/MODIS combination and stacked water vapour models, Int. J. Remote Sens., 30(13), 3343–3363.
[36] Li, Z.H., Fielding, E.J., Cross, P. & Muller, J.-P., 2006b. Interferometric synthetic aperture radar atmospheric correction: GPS topography-dependent turbulence model, J. geophys. Res., 111, B02404, doi:10.1029/2005JB003711.
[37] Li, Z.H., Fielding, E.J., Cross, P. & Muller, J.P., 2006c. Interferometric synthetic aperture radar atmospheric correction: medium resolution imaging spectrometer and advanced synthetic aperture radar integration, Geophys. Res. Lett., 33, L06816, doi:10.1029/2005GL025299.
[38] Li, Z.W., Ding, X.L,Huang, C.,Wadge,G.&Zheng,D.W., 2006d. Modeling of atmospheric effects on InSAR measurements by incorporating terrain elevation information, J. Atmos. Solar-Terres. Phys., 68, 1189–1194
[39] Li, Z. W. W. B. Xu, G. C. Feng, J. Hu, C. C. Wang, X. L. Ding and J. J. Zhu Correcting atmospheric effects on InSAR with MERIS water vapour data and elevation-dependent interpolation model Geophys. J. Int. (2012) 189, 898–910 doi: 10.1111/j.1365-246X.2012.05432.x
[40] Liu, Y., Remote sensing of atmospheric water vapor using GPS data in the Hong Kong region, PhD thesis, The Hong Kong Polytechnic University, Hong Kong, 2000
[41] Mendes, V.B., Modeling the neutral-atmosphere propagation delay in radiometric space techniques, PhD thesis, University of New Brunswick, Fredericton, New Brunswick, Canada, 1999
[42] Mendes, V.B., G. Prates, L. Santos, and R.B. Langley, An evaluation of models for the determination of the weighted mean temperature of the atmosphere, in Proceedings of The Institute of Navigation 2000 National Technical Meeting, pp. 433-438, Anaheim, CA, U.S.A., 26-28 January 2000
[43] Mockler, S.B., Water vapor in the climate system (Special Report, December 1995), American Geophysical Union, Jekyll Island, Georgia, 1995.
[44] Niell, A.E., Preliminary evaluation of atmospheric mapping functions based on numerical weather models, Physics and Chemistry of the Earth, Part A: Solid Earth and Geodesy, 26 (6-8), 475-480, 2001.

[45] Nishihama, M., R. Wolfe, D. Solomon, F. Patt, J. Blanchette, A. Fleig, and E. Masuoka, MODIS Level 1A Earth Location: Algorithm Theoretical Basis Document Version 3.0, pp. 147, the MODIS Science Data Support Team, 1997
[46] Puysségur, B., R. Michel, and J.-P. Avouac (2007), Tropospheric phase delay in interferometric synthetic aperture radar estimated from meteorological model and multispectral imagery,J. Geophys. Res.,112 B05419, doi:10.1029/2006JB004352
[47] Remy,D., Bonvalot, S., Briole, P.&Murakami, M., 2003. Accurate measurements of tropospheric effects in volcanic areas from SAR interferometry data: application to Sakurajima volcano (Japan), Earth planet. Sci. Lett., 213, 299–310.
[48] Saastamoinen, J. (1972). Atmospheric correction for the troposphere and stratosphere in radio ranging of satellites. Geophysics monograph 15, 3rd Int. Symp. Use of Artificial Satellites for Geodesy, AGU, (pp. 247-251)
[49] Schueler, T., A. Pósfay, G.W. Hein, and R. Biberger, A global analysis of the mean atmospheric temperature for GPS water vapor estimation, in Proceedings of ION-GPS 2001, Salt Lake City, Utah, USA, 2001.
[50] Schläpfer, D., C.C. Bore, J. Keller, and K.I. Itten, Atmospheric pre-corrected differential absorption techniques to retrieve columnar water vapor: Application to AVIRIS 91/95 data, in Summaries of the Sixth Annual JPL Airborne Earth Science Workshop, pp. 209-217, JPL, Pasadena (CA), 1995
[51] Webley, P.W., Wadge, G. & James, I.N., 2004. Determining radio wave delay by non-hydrostatic atmospheric modeling of water vapour over mountains, Phys. Chem. Earth, 29, 139–148
[52] Williams, S., Bock, Y. & Fang, P., 1998. Integrated satellite interferometry: tropospheric noise, GPS estimates and implications for interferometric synthetic aperture radar product, J. geophys. Res., 103(B11), 27051–27068. Geosci. Remote Sens., 38(5), 2202–2212
[53] Zebker, H.A., Rosen, P.A. &Hensley, S., 1997. Atmospheric effects in interferometric synthetic aperture radar surface deformation and topographicmaps, J. geophys. Res., 102(B4), 7547–7563